This article has been accepted for publication in a future issue of this journal, but has not been fully edited. Content may change prior to final publication. Citation information: DOI 10.1109/JLT.2017.2787120, Journal of Lightwave Technology

Orbital angular momentum mode converter based on helical long period fiber grating inscribed by hydrogen-oxygen flame

Cailing Fu†, Shen Liu†, Zhiyong Bai, Jun He, Changrui Liao, Ying Wang, Ziliang Li, Yan Zhang, Kaiming Yang, Bin Yu, and Yiping Wang*, *Senior Member, IEEE*

***Abstract*—A high-efficiency grating fabrication method was, for the first time, demonstrated to inscribe helical long period fiber gratings (H-LPFGs) in small numbers by means of twisting a standard single-mode fiber (SMF) during hydrogen-oxygen flame heating and then cutting the helical fiber into in series of sections. Each section of the helical fiber was a desired LPFG whose resonant wavelength, i.e. grating pitch, can be changed by adjusting the twist rate of the helical fiber. The H-LPFG inscribed in a standard SMF could be used to generate orbital angular momentum (OAM) modes, i.e. OAM$_{+1}$ mode, with a purity of 91% and a conversion efficiency of 87% within a large wavelength range from more than the cutoff wavelength of a SMF, which is highly advantageous to all-fiber optical communications based on the OAM mode-division multiplexing technique.**

***Index Terms*—Gratings; Optical vortices; Fiber optics components; Fiber optics communications**

I. Introduction

THE optical orbital angular momentum (OAM) of a light beam has attracted great attention owing to its potential applications in various fields, such as optical fiber communications [1, 2], optical tweezers [3], and detection of rotating objects [4]. Meanwhile, one primary interest of all-fiber optical communication system is to achieve a higher data transmission capacity, which can be realized by use of the mode-division-multiplexing (MDM) technique based on OAM modes [5, 6]. [1]In addition, the existed ways to generate OAM modes are usually based on a cylindrical-lens mode converter [7], a q-plate [8], an integrated silicon device [9], a micrometer-scale meta-reflectarray [10], etc.. Unfortunately, such OAM mode converters have to be free-space coupled with a single-mode fiber (SMF) in order to integrate with a current all-fiber optical communication system, which is disadvantageous to optical communications due to a large free-space-coupling loss. Recently, a few researchers have demonstrated various all-fiber OAM converters, such as a mechanical-microbend-induced long-period fiber grating (LPFG) in a few-mode fiber (FMF) [11], an acoustically induced LPFG in a two-mode fiber (TMF) [12], a CO_2-laser-induced LPFG in a TMF [13], a fiber Bragg grating in an OAM-supporting fiber [14], and a twisted photonic crystal fiber (PCF) [15]. However, such OAM converters were created in special types of fibers, i.e. FMFs, TMFs, and PCFs, rather than in a standard SMF. All of the aforementioned fibers have to be specially designed to generate OAM modes. As a result, they are very expensive and commercially unavailable.

In this letter, we experimentally demonstrated a novel OAM mode converter based on a helical-LPFG (H-LPFG) inscribed in a standard SMF. Such an H-LPFG was inscribed by means of twisting a standard SMF during hydrogen-oxygen flame heating. Moreover, such a LPFG inscription method could be used to fabricate LPFGs in small numbers by means of twisting the fiber once. OAM$_{+1}$ mode was generated and detected by means of the space-free interference between a light through the H-LPFG and a reference beam. Furthermore, the OAM$_{+1}$ mode could be generated within a wide wavelength range from 1520 to 1620 nm by changing the grating pitch of the inscribed H-LPFG.

II. Experimental Results And Discussions

As shown in Fig. 1(a), an experimental setup was designed and built to inscribe an H-LPFG in a standard SMF with a diameter of 125 μm (Corning SMF-28). One end of the employed optical fiber, after removing the coating, was fixed on a translation stage (i.e., translation stage1, Model M-IMS600LM, Newport Corp., USA) via a dual-arm fiber holder. Another end was installed along the central axis of the rotation motor (Model QS-M42, Keyence Corp., Singapore) affixed on another same type of translation stage (i.e., translation stage2). A hydrogen-oxygen flame produced by a hydrogen generator (Model TH-500, China) was used to heat the optical fiber. The rotation motor was employed to twist the optical fiber during hydrogen-oxygen flame heating. A LabVIEW (National Instruments Corp., TX, USA) program with a friendly operational interface was completed to

1 Manuscript received XXXX, 2017; revised XXXX, 2017; accepted XXXX, 2017. Date of publication XXXX, 2017; date of current version XXXX, 2017.

This work was supported by National Natural Science Foundation of China (grant nos. 61425007, 61635007, 61675137 and 61605129), Guangdong Natural Science Foundation (grants nos. 2015B010105007, 2014A030308007 and 2017A010102015), Education Department of Guangdong Province (grant no. 2015KTSCX119), Science and Technology Innovation Commission of Shenzhen (grants nos. JCYJ20160427104925452 and JCYJ20170412105604705), Personal Crew of Science and Technology Program of Shenzhen (GRCK2016082611313201). We acknowledge Prof. Zhaohui Li (Sun Yat-sen University, China) and Dr. Shecheng Gao (Jinan University, China) for providing help during OAM purity measurements.

Cailing Fu, Shen Liu, Zhiyong Bai, Jun He, Changrui Liao, Ying Wang, Ziliang Li, Yan Zhang, Kaiming Yang, Bin Yu, and Yiping Wang are affiliated with Key Laboratory of Optoelectronic Devices and Systems of Ministry of Education and Guangdong Province, College of Optoelectronic Engineering, Shenzhen University, Shenzhen 518060, China.

† Cailing Fu and Shen Liu contributed equally to this work.

(*Corresponding author e-mail: ypwang@szu.edu.cn.)

This article has been accepted for publication in a future issue of this journal, but has not been fully edited. Content may change prior to final publication. Citation information: DOI 10.1109/JLT.2017.2787120, Journal of Lightwave Technology

simultaneously control each device in the experimental setup.

First, the hydrogen-oxygen flame with a heat zone of approximately 1 cm was launched to heat the fiber into a fused status. The two ends of the fiber were then continuously moved along the fiber axis via the translation stage1 with a velocity of v_1 and the translation stage2 with a velocity of v_2, respectively. In our experiments, v_1 and v_2 were set as 1.60 and 1.56 mm/s, respectively. Note that v_1 must be greater than v_2 in order to apply a certain longitudinal stress in the fiber. In addition, the left end of the fiber was twisted with a constant rate of Ω. After twisting the fiber with a rate of Ω=183 rpm for a time of T=50 s, a helical optical fiber with a length of 80 mm and a helical pitch of 524.5 μm was achieved. Note that the total length of the helical fiber was achieved using the equation $L'=v_1*T$, and the helical pitch (Λ), i.e., grating pitch, was calculated using the equation $\Lambda=v_1*60/\Omega$.

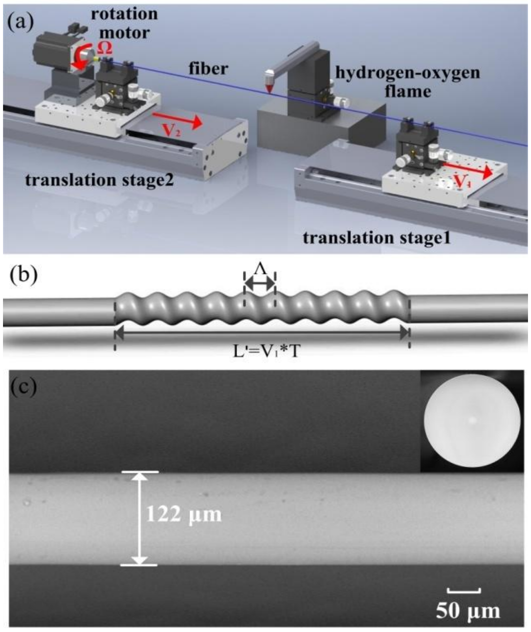

Fig. 1. (a) Schematic diagram of H-LPFG inscription by use of a hydrogen-oxygen flame. (b) Schematic diagram of periodic helical structures solidified in the fiber. (c) Scanning electron micrographs of the side view and cross-section (inset) of an inscribed H-LPFG sample.

As soon as the heated zone of the fiber was moved away from the hydrogen-oxygen flame, periodic helical structures with a fused status were solidified in the fiber, which are schematically illustrated in Fig. 1(b). Thus, periodic residual stress was reserved in the helical fiber. The mechanism of the phenomenon is similar to that of the residual stress induced in the fiber drawn via a drawing tower. As a result, periodic refractive index modulations were induced along the helical fiber axis due to the well-known elastic-optic effect, thus inscribing an H-LPFG. As shown in Fig. 1(c), no physical deformation was observed on the surface of the achieved helical fiber, but the diameter of the fiber decreased from 125 to 122 μm as a result of the velocity difference (0.04 mm/s) between v_1 and v_2.

In order to measure the transmission spectrum evolution of the H-LPFG achieved, as shown in Fig. 2(a), a helical optical fiber with a length of 80 mm and a helical pitch of 524.5 μm was cut step by step to shorten gradually its length by use of a computer-controlled precision cleaving system comprising an optical fiber cleaver (Model FC-6S, Fujikura Ltd., Japan), an industrial CCD camera, and a precision translation stage with a step of 0.1 μm. The industrial CCD camera was employed to simultaneously monitor the desired position on the fiber surface and the cleaving edge of an optical fiber cleaver. Thus, a desired length of the H-LPFG could be obtained with a length accuracy of less than 10 μm. Then, each end of the cut helical fiber, i.e. H-LPFG, was spliced to a SMF in order to measure its transmission spectrum using a broadband amplified spontaneous emission light source with a wavelength range from 1250 to1650 nm and an optical spectrum analyzer (OSA) (Model AQ6370C, Yokogawa Electric Corp., Japan) with a resolution of 0.2 nm. Three resonant dips, i.e. Dip_1, Dip_2, and Dip_3, with an insertion loss of less than 0.2 dB were observed within the wavelength range from 1250 to 1650 nm. While the grating length increases from 8.4 to 16.8 mm (i.e. from 16 grating periods to 32 grating periods), as shown in Fig. 2(b), the resonant wavelength, corresponding to Dip_1, of the H-LPFG with a grating pitch of 524.5 μm shifts from 1553.0 to 1550.6 nm due to negative refractive index modulation induced by elastic-photo effect in the twisted fiber, and the maximum attenuation at the resonant wavelength increases from -3.2 to -34.9 dB. The phenomenon is similar to the transmission spectrum evolution of the CO_2-laser-induced LPFG observed with an increase of the exposure time [16-19], which confirms that a section of the helical fiber is actually a desired LPFG.

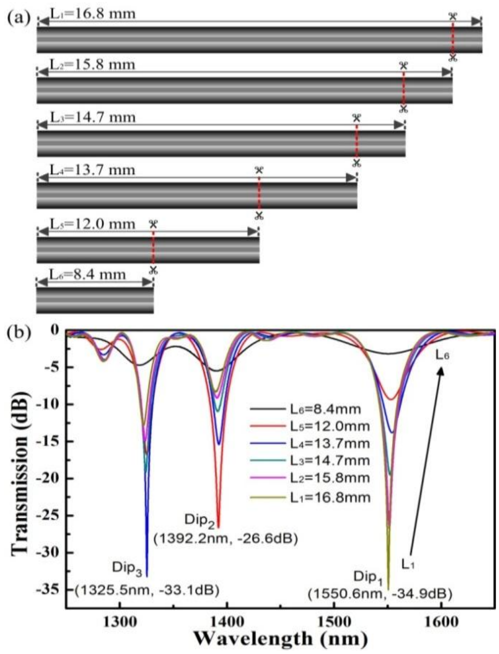

Fig. 2. (a) Schematic diagram of the process for cutting the H-LPFG with a grating pitch of 524.5 μm to decrease the number of grating periods. (b) Transmission spectrum evolution of the H-LPFG with a grating length decrease from 16.8 to 8.4 mm (i.e. number of grating periods).

Another helical fiber sample with a total length of 160 mm and a helical pitch of 527.4 μm was fabricated with parameters of v_1=1.60 mm/s and T=100 s by use of the experimental setup illustrated in Fig. 1.(a). As shown in Fig. 3.(a), the helical fiber sample was cut into a series of H-LPFGs ($H\text{-}LPFG_1'$, $H\text{-}LPFG_2'$, $H\text{-}LPFG_3'$, …, and $H\text{-}LPFG_m'$) with a length of L_1', L_2', L_3', …, and L_m',

This article has been accepted for publication in a future issue of this journal, but has not been fully edited. Content may change prior to final publication. Citation information: DOI 10.1109/JLT.2017.2787120, Journal of Lightwave Technology

respectively, by use of the computer-controlled precision cleaving system mentioned above. Figure 3 (b) illustrates the transmission spectra of H-LPFG$_1$', H-LPFG$_2$', and H-LPFG$_3$' with a length of 16.6, 16.0, and 16.9 mm, respectively. And each H-LPFG sample has a low insertion loss of less than 0.2 dB and a maximum attenuation of more than - 30 dB. This indicates that a few high-quality LPFGs were achieved by means of cutting the helical fiber. In other words, H-LPFGs can be inscribed in small numbers by means of twisting a SMF once during hydrogen-oxygen flame heating, which is a great advantage over other grating inscription methods [20-22]. In our experiments, a helical fiber with a length of about 300 mm and a uniform diameter within the total fiber length has been fabricated in a short time of 188 s using the experimental setup illustrated in Fig. 1(a). Then, fifteen H-LPFGs were obtained in small numbers by means of cutting the helical fiber into a series of sections with a length of approximately 20 mm. And high efficiency and good repeatability of the H-LPFG fabrication method above was proved in our experiments.

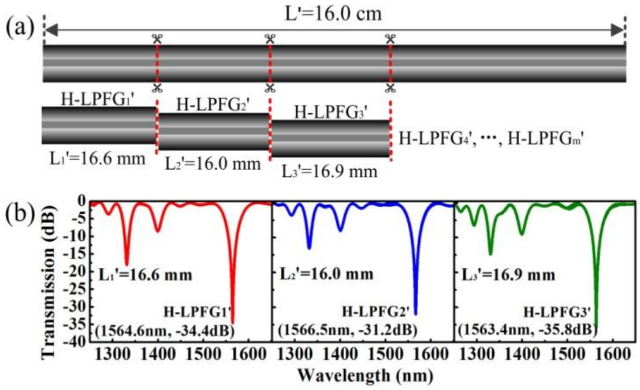

Fig. 3. (a) Schematic diagram of achieving different H-LPFG samples by cutting a helical optical fiber. (b) Transmission spectra of H-LPFG$_1$, H-LPFG$_2$, and H-LPFG$_3$.

To investigate the phase matching condition as a function of the resonant wavelength, six helical fiber samples (H-LPFG$_1$, H-LPFG$_2$, …, and H-LPFG$_6$) with the same number of grating periods (i.e. 32 grating periods) and different grating pitches of 533.3, 524.5, 516.1, 507.9, 500.0, and 492.3 μm were fabricated by applying a twist rate of 180, 183, 186, 189, 192, and 195 rpm, respectively. Figure 4 (a) illustrates that each H-LPFG has three attenuation dips (Dip$_1$, Dip$_2$, and Dip$_3$) with a low insertion loss of less than 0.2 dB. And Dip$_1$ of each H-LPFG has a large coupling strength of more than - 32dB at the resonant wavelength. As shown in Fig. 4.(b), the measured resonant wavelength was shifted toward a longer wavelength with the increase of grating pitch, which is the same trend exhibited in conventional laser-induced LPFGs [23, 24]. This phenomenon confirms again that each section of the helical fiber is actually a desired LPFG. And high-quality H-LPFGs with a desired resonant wavelength can be realized by changing the twist rate of the fiber.

An experimental setup illustrated in Fig. 5.(a) was demonstrated to detect the OAM modes generated by our H-LPFGs illustrated in Fig. 4.(a). Light from a tunable laser (Model 81940A, Agilent Technologies, Santa Clara, CA, USA) with a wavelength range from 1520 to 1620 nm was divided into two parts by a fiber coupler (90:10). One part of the light (90%) was propagated into an achieved H-LPFG to generate OAM modes and then collimated into a beam splitter (BS) through a lens (Lens1). The H-LPFG sample was cleaved at the last grating period to detect the generated OAM mode. Another part of the light (10%) was propagated into a polarization controller (PC) and an attenuator, and then collimated into the BS through another lens (Lens2) as a reference beam. The intensity of the reference beam was controlled to achieve clear interference patterns by the tunable attenuator. The generated OAM modes from the H-LPFG interfered with the reference beam on the BS. The beam profile and interference pattern of the generated OAM can be observed by use of an infrared CCD (Model 7290A, Electrophysics Corp.).

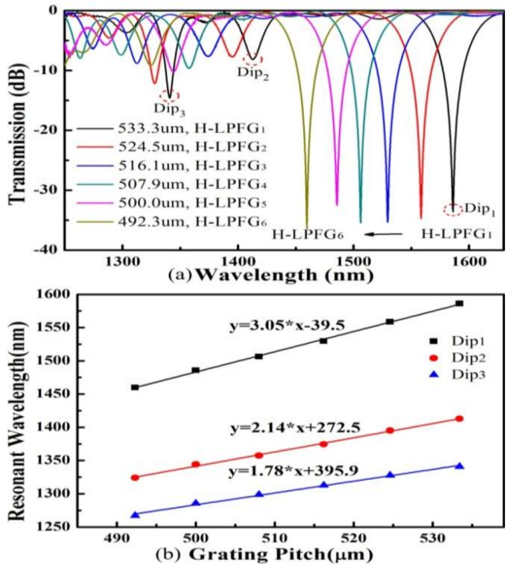

Fig. 4. (a) Transmission spectra of six H-LPFG samples with grating pitches of 533.3, 524.5, 516.1, 507.9, 500.0, and 492.3 μm. (b) Measured resonant wavelengths of the H-LPFGs versus grating pitch.

Without the reference beam, as shown in Figs. 5(b) and 5(d), the near-infrared mode beam profile of H-LPFG$_1$ and H-LPFG$_3$, illustrated in Fig. 4.(a), with a resonant wavelength of 1586 and 1530 nm, respectively, had a clear annular shape in the center. In order to verify the characteristic of a helical phase, the generated OAM mode was interfered with the reference beam. Consequently, as shown in Figs. 5(c) and 5(e), the anticlockwise spiral interference patterns for the OAM$_{+1}$ mode, corresponding to H-LPFG$_1$ and H-LPFG$_3$, at resonant wavelengths of 1586 and 1530 nm were clearly observed, indicating that the OAM$_{+1}$ mode was successfully generated at the output end of the H-LPFGs. Moreover, our H-LPFGs could be used to generate high-quality OAM modes within a large wavelength range from more than the cutoff wavelength of a SMF. Currently, the OAM modes were experimentally generated within the wavelength range from 1520 to 1620 nm by means of changing the pitch of the H-LPFGs due to the wavelength range limit of our current tunable laser. As well-known, the incident beam from the tunable laser does not carry any OAM. The OAM of light was excited at the output of the twisted fiber, i.e. H-LPFG, resulting from helical structure with single-helix rotational symmetry in the cross section of the fiber [25].

This article has been accepted for publication in a future issue of this journal, but has not been fully edited. Content may change prior to final publication. Citation information: DOI 10.1109/JLT.2017.2787120, Journal of Lightwave Technology

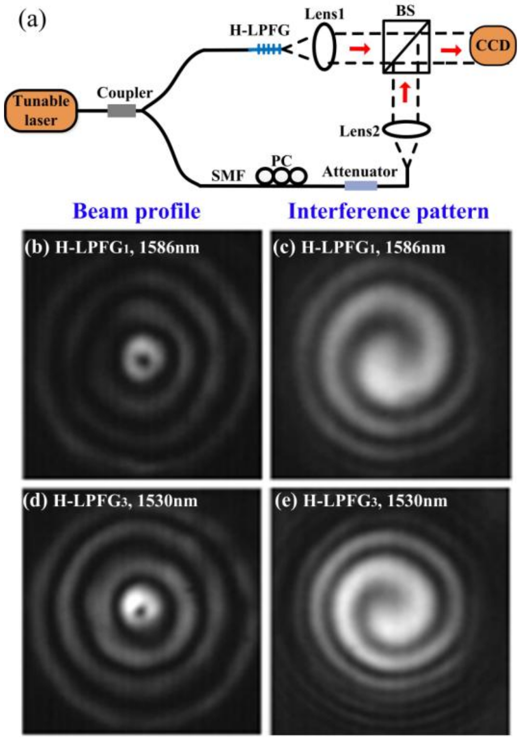

Fig. 5. (a) Schematic diagram of experimental setup for detecting the OAM modes generated by the inscribed H-LPFG. (b),(c),(d),(e) Beam profiles (left) and interference patterns (right) of the OAM_{+1} mode generated by the inscribed $H\text{-}LPFG_1$ and $H\text{-}LPFG_3$ at the wavelength of 1586 and 1530 nm, respectively.

As shown in Fig. 6.(a), the purity of the generated OAM mode in the inscribed helical fiber grating, e.g. $H\text{-}LPFG_1$, was measured to investigate further the characterization of the OAM by use of mode decomposition method based on holograms [26,27]. The forked holograms were generated by a reflective phase-only liquid crystal spatial light modulator (LC-SLM, holoeye). Only the first order diffraction was passed through an aperture. A lens with a long focal length of 20 cm and an infrared CCD (Model 7290A, Electrophysics Corp.) were employed to observe the far-field beam profile. The first-order diffraction beam from a forked grating with an order of l has an added helical phase, exp(ilθ). A forked hologram with l=-1 was applied to convert the OAM mode with l=1 to LP_{01} mode. Then, as shown in Fig. 6.(b), a series of forked grating holograms (l = −2, −1, 0, +1, +2) were applied to observe the beam profile of the conjugate OAM mode. The modal contribution of each OAM mode was measured by recording the power in the center of the corresponding beam profile illustrated in Fig. 6.(b). We calculated the relative power of the generated OAM modes. As shown in Fig. 6.(c), the representative data demonstrated that l=+1 mode of the generated OAM modes is primary, and the purity of OAM_{+1} mode is 91%. Furthermore, $H\text{-}LPFG_1$ has a low insertion loss of less than 0.2 dB and a high coupling efficiency of - 32.5 dB at the resonant wavelength of 1586.1 nm, thus its conversion efficiency from the core mode to OAM_{+1} mode is up to 87%.

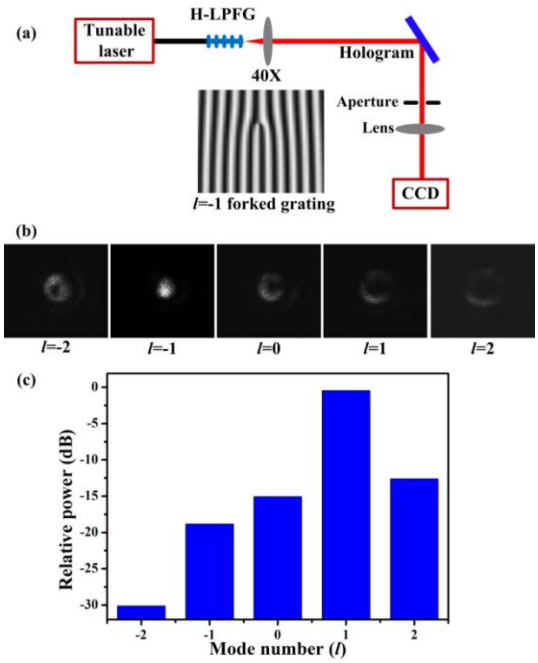

Fig. 6. (a) Experimental setup for measuring the purity of the OAM mode generated by the inscribed H-LPFG; (b) Beam profiles of the generated OAM mode pattern when a series of forked holograms (l = −2, −1, 0, +1, +2) were applied; (c) Calculated relative power of the generated OAM modes.

In order to investigate the polarization characteristics of our H-LPFGs, a tunable laser (Agilent Model 81940A), a polarization synthesizer (Agilent Model N7786B), and an optical power meter (Agilent Model N7744A) were employed to measure the polarization-dependent loss (PDL) of a H-LPFG with a resonant wavelength of 1578.0 nm and a maximum attenuation of - 26.7 dB. As shown in Fig. 7., the H-LPFG has a maximum PDL of 3.0 dB around the resonant wavelength, resulting from the asymmetric azimuthal profile of refractive index modulation in the H-LPFG.

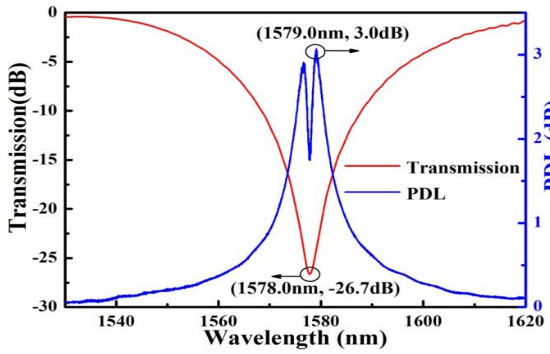

Fig. 7. Measured transmission spectrum (red) and PDL (blue) of the H-LPFG with a grating pitch of 533.3 μm.

III. Conclusion

In conclusion, high-quality H-LPFGs were fabricated in small numbers by twisting a standard SMF with a fused status and then cutting the helical fiber into a series of sections. Each section of helical fiber is an ideal LPFG whose resonant wavelength, i.e. grating pitch, can be changed by adjusting the twist rate of the helical fiber. OAM_{+1} modes were experimentally generated at wavelengths of 1530 and 1586 nm using the H-LPFG inscribed in a standard SMF. The OMA_{+1} mode exhibits a purity of 91% and a conversion efficiency of 87%. Moreover, such a H-LPFG can be used to generate OAM_{+1} modes within a large wavelength range from more than the cutoff wavelength of a SMF, which have important applications based on OAM mode-division multiplexing in all-fiber optical communications.

REFERENCES

[1] N. Ahmed, Z. Zhao, L. Li, H. Huang, M. P. Lavery, P.C. Liao, Y. Yan, Z. Wang, G. D. Xie, Y. X. Ren, A. Almaiman, A. J. Willner., S. Ashrafi, A. F. Molisch, M. Tur, and A. E.Willner, "Mode-Division-Multiplexing of Multiple Bessel-Gaussian Beams Carrying Orbital-Angular-Momentum for Obstruction-Tolerant Free-Space Optical and Millimetre-Wave Communication Links," *Sci Rep*, vol. 6, pp. 22082, 2016.

[2] H. L. Li, D. B. Phillips, X. Y. Wang, Y.-L. D. Ho, L. F. Chen, X. Q. Zhou, J. B. Zhu, S. Y. Yu ,and X. L. Cai, " Orbital angular momentum vertical-cavity surface-emitting lasers," *Optica*, vol. 2, no. 6, pp. 547-552, 2015.

[3] C. T. Schmiegelow, J. Schulz, H. Kaufmann, T. Ruster, U. G. Poschinger, and F. Schmidt-Kaler, "Transfer of optical orbital angular momentum to a bound electron," *Nat. Commun.*, vol. 7, pp. 12998, 2016.

[4] M. P. J. Lavery, F. C. Speirits, S. M. Barnett ,and M. J. Padgett, "Detection of a Spinning Object Using Light's Orbital Angular Momentum," *Science* ,vol. 341, pp. 537-540, 2013.

[5] H. Huang, G. Milione, M. P. J. Lavery, G. D. Xie, Y. X. Ren, Y. W. Cao, N. Ahmed, T. An Nguyen, D. A. Nolan, M. J. Li, M. Tur, R. R. Alfano, and A. E. Willner," Mode division multiplexing using an orbital angular momentum mode sorter and MIMO-DSP over a graded-index few-mode optical fibre," *Sci Rep*, vol. 5, pp. 14931, 2015.

[6] Y. Li, J. Deng, J. Li ,and Z. Li., "Sensitive orbital angular momentum monitoring by using gradually changing-period phase grating in OAM-multiplexing optical communication systems," *IEEE Photon. J.*, vol. 8, no. 2, pp. 7902306, 2016.

[7] M. J. Padgett , and L. Allen, "Orbital angular momentum exchange in cylindrical-lens mode converters," *Journal of Optics B: Quantum and Semiclassical Optics*, vol. 4, pp. s17-s19, 2002.

[8] D. Naidoo, F. S. Roux, A. Dudley, I. Litvin, B. Piccirillo, L. Marrucci, and A. Forbes, "Controlled generation of higher-order Poincaré sphere beams from a laser", *Nat. Photonics*, vol. 10, pp. 327, 2016.

[9] X. L. Cai, J.W. Wang, M. J. Strain, B. Johnson-Morris, J. B. Zhu, M. Sorel, J. L. OBrien, M. G. Thompson, S. Y. Yu, "Integrated Compact Optical Vortex Beam Emitters," *Science*, vol. 338, pp. 363, 2012.

[10] J. P. Liu, C. J. Min, T. Lei, L. P. Du, Y. S. Yuan, S. B. Wei, Y.P. Wang ,and X. C. Yuan, "Generation and detection of broadband multichannel orbital angular momentum by micrometer-scale meta-reflectarray," *Opt. Express*, vol. 24, no. 1, pp. 212-218, 2016.

[11] S. H. Li, Q. Mo, X. Hu, C. Du ,and J. Wang, "Controllable all-fiber orbital angular momentum mode converter," *Opt. Lett.*, vol. 40, no. 18, 4376-4379, 2015.

[12] W. D. Zhang, K. Y. Wei, L. G. Huang, D. Mao, B. Q. Jiang, F. Gao, G. Q. Zhang, T. Mei ,and J. L. Zhao, "Optical vortex generation with wavelength tunability based on an acoustically-induced fiber grating," *Opt. Express*, vol. 24, no. 17 19278-19285, 2016.

[13] Y. H. Zhao, Y. Q. Liu, L. Zhang, C. Y. Zhang, J. X. Wen ,and T. Y. Wang, "Mode converter based on the long-period fiber gratings written in the two-mode fiber," *Opt. Express*, vol. 24,no. 6, pp. 6186-6195, 2016.

[14] L. Wang, P. Vaity, B. Ung, Y. Messaddeq, L. A. Rusch ,and S. LaRochelle, "Characterization of OAM fibers using fiber Bragg gratings," *Opt. Express*, vol. 22, no. 13, pp. 15653-15661, 2014.

[15] G. K. L. Wong, M. S. Kang, H. W. Lee, F. Biancalana, C. Conti, T. Weiss, P. St. J. Russell, "Excitation of Orbital Angular Momentum Resonances in Helically Twisted Photonic Crystal Fiber," *Science*, vol. 337, pp. 446-449, 2012.

[16] Y. P. Wang, D. N. Wang, W. Jin, Y. J. Rao ,and G. D. Peng, "Asymmetric LPFG fabricated by CO2 laser to carve periodic grooves on the optical fiber," *Appl. Phys. Lett.* ,vol. 89, no. 15, pp. 151105, 2006.

[17] G. L. Yin, C. R. Liao, J. T. Zhou, X. Y. Zhong, G. J. Wang, B. Sun, and J. He, "Long period fiber gratings inscribed by periodically tapering a fiber," *IEEE Photon. Technol. Lett.*, vol. 26, no. 7, pp.698-701, 2014.

[18] Y. P. Wang, W. Jin, J. Ju, H. F. Xuan, H. L. Ho, L. M. Xiao, and D. N. Wang, " Long period gratings in air-core photonic bandgap fibers," *Opt. Express*, vol. 16, no. 4,pp. 2784-2790, 2008.

[19] Y. P. Wang, Y. J. Rao, Z. L. Ran, T. Zhu, and A. Z. Hu, "A Novel Tunable Gain Equalizer Based on a Long-Period Fiber Grating Written by High-Frequency CO_2 Laser Pulses," *IEEE Photon. Technol. Lett.*, vol. 15, no. 2, pp.251-253, 2003.

[20] G. Inoue, P. Wang ,and H. P. Li, "Flat-top band-rejection filter based on two successively-cascaded helical fiber gratings," *Opt. Express*, vol. 24, no. 5, pp. 5442-5447, 2016.

[21] S. Oh, K. R. Lee.U. Paek, and Y. Chung, "Fabrication of helical long-period fiber gratings by use of a CO_2 laser," *Opt. Lett.*, vol. 29, no. 13 pp. 1464-1466,2004.

[22] Y. P. Wang, "Review of long period fiber gratings written by laser," *J. Appl. Phys.*, vol. 108, pp. 081101, 2010.

[23] X. Y. Zhong, Y. P. Wang, C. R. Liao, G. L. Yin, J. T. Zhou, G. J.Wang, B. Sun, and J. Tang, "Long Period Fiber Gratings Inscribed With an Improved Two-Dimensional Scanning Technique," *IEEE Photon. J.* ,vol. 6, no. 4,pp. 2201508, 2014.

[24] F. Esposito, R. Ranjan, S. Campopiano ,and A. Iadicicco, "Experimental Study of the Refractive Index Sensitivity in Arc-induced Long Period Gratings," *IEEE Photon. J.*, vol. 9,no. 1, pp. 7100110, 2017.

[25] H. X. Xu, L. Yang." Conversion of orbital angular momentum of light in chiral fiber gratings,". *Opt. Lett.*, vol. 38, no. 11, pp.1978-80, 2013.

[26] R. D. Niederriter, M. E Siemens, J. T. Gopinath, " Continuously tunable orbital angular momentum generation using a polarization-maintaining fiber, " *Opt. Lett*., vol. 41, no. 14 , pp. 3213, 2016.

[27] Y. J. Li, L. Jin, H. Wu, S. C. Gao, Y. H. Feng, and Z. H. Li, "Superposing multiple LP modes with micro phase difference distributed along fiber to generate OAM mode". *IEEE Photonics Journal*, vol. 9, no. 2, pp. 7200909, 2017.

Cailing Fu was born in Hubei, China, in 1989. She received the M.S. degree in optical engineering from Wuhan Institute of Technology, Wuhan, China, in 2015. She is currently pursuing the Ph.D. degree in optical engineering at Shenzhen University, Shenzhen, China.

Shen Liu was born in Henan, China, in 1986. He received his Ph.D. degree in optical engineering from Shenzhen University, China, in 2017. His current research interest focus on optical fiber sensors and devices.

Zhiyong Bai received the B.S. degree in physics from Ningbo university in 2008, the M.S. degree in optics from South China normal university in 2011, and the Ph.D. degree in optics in Nankai university in 2014. From 2014 to 2015, he has with the State Grid Electric Power Research Institute as a R&D engineer. Since 2015, he has been a Postdoctoral Research Fellow at the Guangdong and Hong Kong Joint Research Centre for Optical Fiber Sensors, Shenzhen University, China. His current research interests include optical fiber gratings, orbital angular momentum, and optical fiber sensors. He is the author or coauthor of more than 30 journal papers.

Jun He was born in Hubei, China, in 1985. He received the B.Eng. degree in electronic science and technology from Wuhan University, Wuhan, China, in 2006 and the Ph.D. degree in electrical engineering from the Institute of Semiconductors, Chinese Academy of Sciences (CAS), Beijing, China, in 2011. From 2011 to 2013, he was with Huawei Technologies, Shenzhen, China, as a Research Engineer. From 2013 to 2015, he was with Shenzhen University, Shenzhen, China, as a Postdoctoral Research Fellow. From 2015 to 2016, he was with The University of New South Wales (UNSW), Sydney, Australia, as a Visiting Fellow. Since 2017, he has been in Shenzhen University, Shenzhen, China, as an Assistant Professor. His current research interests focus on optical fiber sensors, fiber Bragg gratings (FBGs), and fiber lasers. He has

This article has been accepted for publication in a future issue of this journal, but has not been fully edited. Content may change prior to final publication. Citation information: DOI 10.1109/JLT.2017.2787120, Journal of Lightwave Technology

authored or coauthored 4 patent applications and more than 50 journal and conference papers. Dr. He is a member of the Optical Society of America.

Changrui Liao was born in Shandong, China, in 1984. He received the B.Eng. degree in optical engineering and the M.S. degree in physical electronics from Huazhong University of Science and Technology (HUST), Wuhan, China, in 2005 and 2007, respectively, and the Ph.D. degree in electrical engineering from the Hong Kong Polytechnic University, Hong Kong, in 2012. He is currently with Shenzhen University, Shenzhen, China, as an Associate Professor. His current research interests focus on femtosecond laser micromachining, optical fiber sensors, and opto microfluidics.

Ying Wang was born in Henan, China, in 1983. He received the B.S. degree in applied physics and the Ph.D. degree in physical electronics from Huazhong University of Science and Technology (HUST), Wuhan, China, in 2004 and 2010, respectively. From 2010 to 2015, he worked in the Department of Electrical Engineering in the Hong Kong Polytechnic University, Hong Kong, China, as a research associate. Since 2015, he has joined in the College of Optoelectronic Engineering, Shenzhen University, China, as a lecturer. His research interests are optical fiber sensors and femtosecond laser micromachining.

Ziliang Li was born in Hunan, China, in 1994. He received the B.S. degree from Jiangsu University in 2016. He is currently completing his master degree in Shenzhen University, Shenzhen, China.

Yan Zhang was born in zhenghzou, China, in 1992. He received the B.S. degree in School of physics and chemistry from Henan Polytechnic University, in 2016. He is now a postgraduate student in Shenzhen University, China. His current research interests focus on long period fiber grating and chiral fiber grating.

Kaiming Yang was born in Jiangxi, China, in 1990. He received the B.S. degree in optical information science and Technology from East China JiaoTong University, in 2012. He is now a Ph.D. candidate in Shenzhen University, China. His current research interests focus on fiber Bragg gratings and femtosecond laser micromachining.

Bin Yu was born in Jiangsu, China, in 1976. He received the B.Eng. degree from Changchun University of Science and Technology, China, in 1998. He received the M.S. degree and the Ph.D. degree from Changchun Institute of Optics, Fine Mehcanics and Physics, Chinese Academy of Sciences (CAS),Changchun ,China, in 2000 and 2003, respectively. From 2003 to 2005, he was with Tianjin University and Shenzhen enterprise station, China, as a Postdoctoral Fellow. From 2005-2006, he was with the Centre national de la recherche scientifique (CNRS) as a Postdoctoral Fellow. Since 2007, he has been with Shenzhen University, Shenzhen, China, as a Professor. His current research interests focus on nanometer resolution fluorescence microscopy imaging, nanowire light source and diffraction optics.

Yiping Wang (SM'11) was born in Chongqing, China, in 1971. He received the B.Eng. degree in precision instrument engineering from Xi'an Institute of Technology, China, in 1995 and the M.S. degree and Ph.D. degree in optical engineering from Chongqing University, China, in 2000 and 2003, respectively. From 2003 to 2005, he was with Shanghai Jiao Tong University, China, as a Postdoctoral Fellow. From 2005 to 2007, he was with the Hong Kong Polytechnic University, as a Postdoctoral Fellow. From 2007 to 2009, he was with the Institute of Photonic Technology (IPHT), Jena, Germany, as a Humboldt Research Fellow. From 2009 to 2011, he was with the Optoelectronics Research Centre (ORC), University of Southampton, U.K., as a Marie Curie Fellow. Since 2012, he has been with Shenzhen University, Shenzhen, China, as a Distinguished Professor. His current research interests focus on optical fiber sensors, fiber gratings, and photonic crystal fibers. He has authored or coauthored 1 book, 21 patent applications, and more than 240 journal and conference papers. Prof. Wang is a Senior Member of IEEE, the Optical Society of America, and the Chinese Optical Society.